Phase equilibria and solidification of Mg-rich Al-Mg-Si alloys

Rocio Valdés, Alexandre Freulon, Jean-Baptiste Deschamps, Ma Qian, Jacques Lacaze

Phase equilibria and solidification of Mg-rich Al-Mg-Si alloys

R. Valdes[1], A. Freulon[1], J.-B. Deschamps[1], Ma Qian[2], J. Lacaze[1]
1- CIRIMAT, UMR 5085, ENSIACET, 31077 Toulouse cedex 4, France
2- Brunel Centre for Advanced Solidification Technology, Brunel University, UB8 3PH, UK
Contact: jacques.lacaze@ensiacet.fr

Keywords: Al-Mg-Si alloys; Solidification; Phase equilibria; Differential thermal analysis

Abstract. The solidification and solid-state phase equilibria of four Al-Mg-Si alloys containing 30-70%Mg and 0.5-3.5%Si, selected on the basis of an isothermal section of the Al-Mg-Si system calculated at 300 °C, have been investigated. Solidification paths of Mg-rich Al-Mg-Si alloys finish on ternary eutectics and the temperatures of two of these eutectic reactions, i.e. L↔(Al)+β+ Mg_2Si and L↔(Mg)+γ+ Mg_2Si, have been determined to be at ~ 448 °C and ~ 436 °C respectively by DTA. The characteristic temperatures recorded on the DTA curves are analysed and a linear relationship is found between the peak temperature and the square root of the scanning rate.

Introduction

Aluminium and magnesium alloys containing silicon are well known for their age hardening characteristics. Owing to their good castability, they are of high industrial relevance. Although increasing demand for higher strength and better service properties has led to the development of more complex alloys, the Al-Mg-Si system remains of great importance for understanding the solidification and heat-treatment of many relevant industrial alloys. While there are a few studies available related to the liquidus surface of this system and quite a lot on solid-state equilibria in the Al corner, very scarce information deals with Mg-rich alloys, in particular the solid-state equilibria in the Mg corner. The present study was intended to check available descriptions of the Al-Mg-Si phase diagram against new experimental results on high Mg alloys in the Al-Mg-Si system.

Experimental details and characterisation of the as-cast alloys

Fig. 1 shows an isothermal section of the Al-Mg-Si phase diagram calculated at 300 °C using a new set of optimised parameters presented elsewhere [1] based on the COST 507 [2] data bank. The bold lines are limits between various domains, where the phases present are indicated on the right-hand side of the diagram. (Al) and (Mg) stand for the fcc and hcp solid solutions rich in Al and Mg respectively, while $Al_{30}Mg_{23}$ (ε), Al_3Mg_2 (β) and $Al_{12}Mg_{17}$ (γ) are compounds from the binary Al-Mg system. Three alloy compositions, shown as crosses in Fig. 1, were chosen from three different phase fields along the interrupted line. A fourth alloy, much closer to the Al-Mg side (see square in Fig. 1), was also prepared for this study. Table 1 lists the nominal compositions of these alloys.

Samples taken out from the as-cast ingots were prepared by standard metallographic techniques and first observed by optical microscopy. Figs. 2(a) to 2(d) show typical views of the microstructure of each alloy. The phases observed were ascertained by chemical microanalysis and X-ray diffraction (XRD), as will be detailed later. In each alloy, the primary phase appears as faceted dark crystals of Mg_2Si. This is in agreement with the liquidus surface of the Al-Mg-Si system. Alloy D30, which contains only 0.5 wt.% Si, shows much less primary Mg_2Si crystals. In alloys A30 and D30 which both contain 30 wt.% Mg, (Al) dendrites are seen enveloped within a matrix of β. Alloy D30 shows a finer microstructure because its cooling rate was higher than the cooling rates for the other alloys. Numerous small dark precipitates, which present the same contrast as primary Mg_2Si, were found within the β phase in alloy D30 (Fig. 2(a)). Similar precipitates were also seen in alloy A30 but they were much less in quantity and generally located close to the (Al) phase. It is unclear if these precipitates are associated with the expected ternary eutectic (liquid↔(Al)+β+ Mg_2Si) or if they form during cooling after solidification finishes. This will be addressed subsequently.

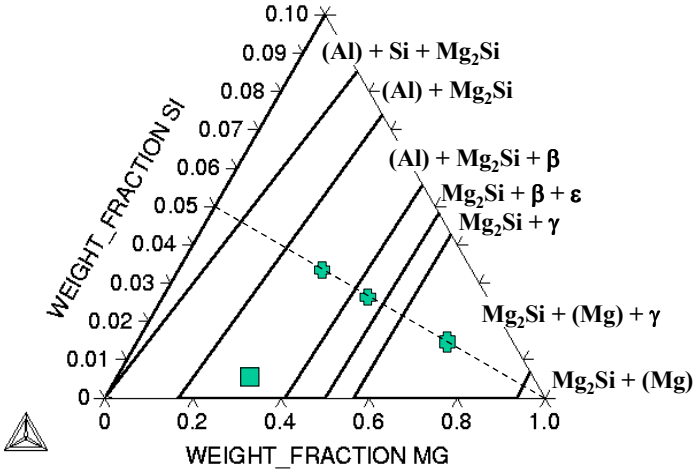

Figure 1 - Isothermal section of the Al-Mg-Si system at 300 °C.

Table 1 - Nominal composition of the alloys studied (wt %).

Alloy table	Al	Mg	Si
A30	66.5	30.0	3.5
A45	52	45	3
A70	28	70	2
D30	69.5	30	0.5

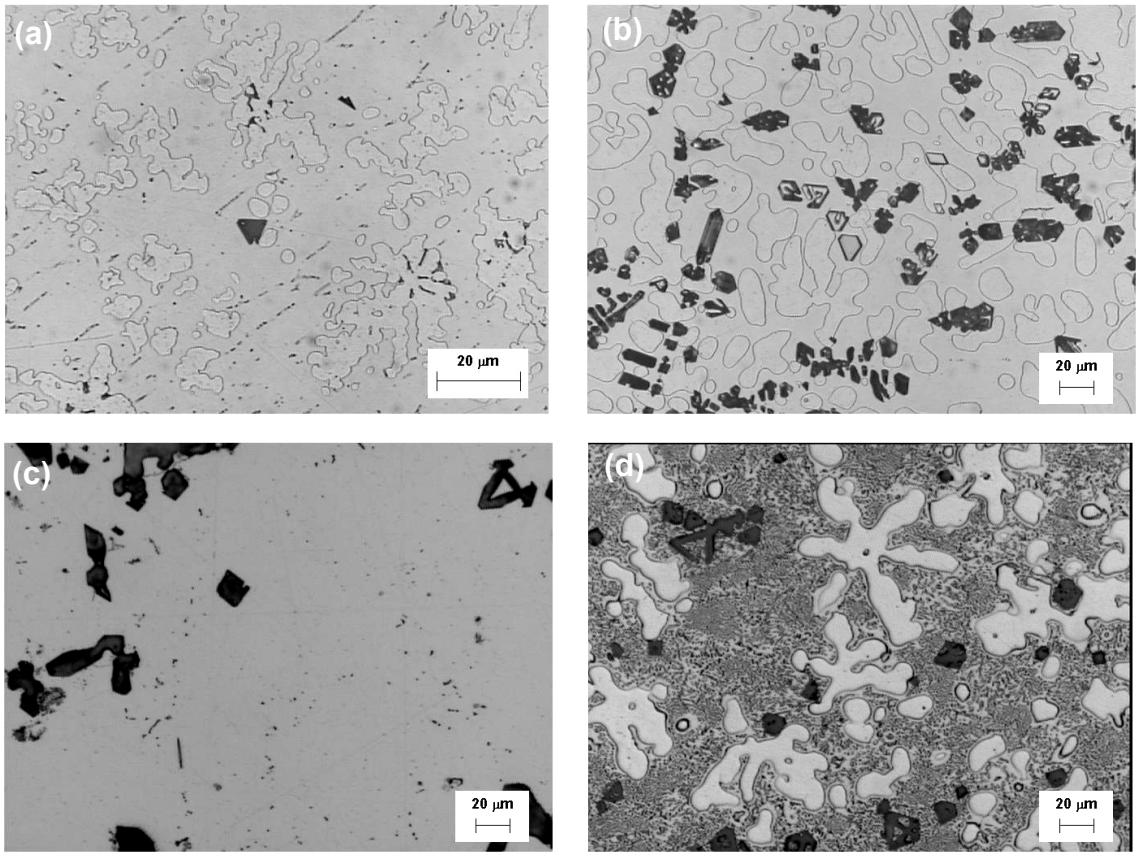

Figure 2 - Optical micrographs of the as-cast microstructures of the four alloys studied: (a) D30; (b) A30; (c) A45; (d) A70. Alloys A30, A45 and D30 were etched with Keller's reagent while alloy A70 with a solution of 0.5 % HNO_3 in etanol.

In addition to primary Mg_2Si crystals, alloy A45 is essentially made of the γ phase. Also observed are some fine precipitates similar to those found in alloys D30 and A30. Apart from blocky precipitates of Mg_2Si, well-developed dendrites of the (Mg) phase are observed in the microstructure of alloy A70. These dendrites are surrounded by a halo of the $Al_{12}Mg_{17}$-γ phase and the remaining volume is occupied by a rod-like eutectic made of γ and (Mg) phases. However, the presence of Mg_2Si was not resolved within this eutectic, which should be the terminal three phase

(Mg_2Si+(Mg)+γ) eutectic. An estimate of the eutectic composition was made by EDS analysis on areas of 30µm × 40µm and was found to be ~ 30.1 wt.% Al and ~ 69.9 wt.% Mg.

X-ray diffraction analyses of the four alloys were performed with a Seifert 2000 apparatus equipped with a Cu cathode ($\lambda_{K\alpha}$=1.540598 Å) and operated at 40 kV and 30 mA. Indexing of the different XRD patterns was made with the software Carine v.3.1 [3] according to the information given in Pearson's handbook [4]. It was found that only phases expected from the stable phase diagram were present. Each alloy was subjected to differential thermal analysis (DTA) using a SETSYS apparatus from SETARAM. The DTA signal was recorded on heating and cooling with various scanning rates, 2.5, 5 and 10 $K.min^{-1}$. The scanning rates used for heating and cooling were the same and a new sample was used in each run. The DTA samples thus obtained were then prepared for metallographic observations. Scanning electron microscopy (SEM) was performed by means of an LEO scanning electron beam microscope operated under 15 kV. Microanalysis was achieved with an energy dispersive spectrometer IMIX from PGT, using pure elements as standards. For microanalysis, the probe current was maintained at 1.5 nA and the spectra were cumulated during 200 seconds.

A diffusion couple with an Al-5wt%Si alloy (cast at DLR Germany) on one side and alloy A70 on the other side was prepared and introduced in an ampoule sealed under low argon pressure. It was then maintained at 300 °C for 7 months to allow equilibrium at the junction.

Diffusion couple

Fig. 3 presents an SEM micrograph across the junction of the diffusion couple, demonstrating the microstructural changes that have taken place after 7 months at 300°C. The phases identified according to EDS analyses are indicated on the micrograph. The initial location of the junction contains many large pores. On the outmost part of the Al-Si side, silicon lamellae appear white in the (Al) matrix. Close to the junction, these lamellae are replaced by Mg_2Si precipitates with grey contrast. On the other side of the couple, the three Al-Mg compounds, β, ε and γ, appear in a sequence with an increase in the Mg content. The microstructure in the zone at the outmost right-hand side of the micrograph is composed of dark dendrites of the (Mg) phase in a matrix of γ and some large faceted crystals of Mg_2Si, where these Mg_2Si crystals are invisible due to the poor contrast with the γ phase in backscattered imaging mode. Similar Mg_2Si precipitates were present together with β and γ but not in the zone with ε. The dark spots in the γ+Mg_2Si zone are pores.

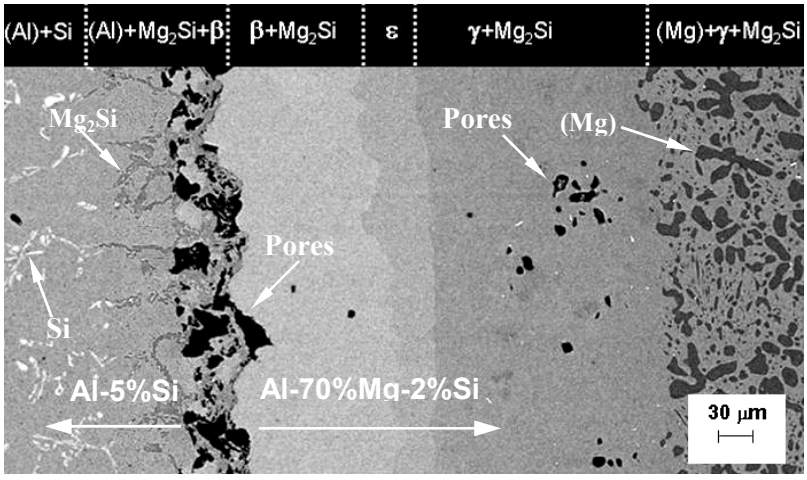

Figure 3 – SEM micrograph showing the junction of the diffusion couple after 7 months at 300 °C (backscattered electron imaging).

The composition across the inter-diffusion zone was estimated by means of line profiles with spot measurements made at every 3 µm in spacing. Mg_2Si was found to have the same composition

in whatever equilibrium it is involved. Also, the amount of silicon was found to be less than 0.1wt% in any of the three Al-Mg compounds (ε, β and γ) and in each of the (Al) and (Mg) phases as well. The very low silicon content in the ε phase was also confirmed with WDS in an electron probe microanalyser. Based on these quantitative analyses, the compositions of the various phases at the boundary of each microstructural zone were carefully evaluated, giving estimates of the tie-lines in three phase equilibria (two phases from the Al-Mg system plus Mg_2Si). These compositions are reported in Table 2 with the silicon content being set at zero. Since the amount of silicon that may enter the Al-Mg compounds (ε, β and γ) is very low, it is expected that the composition of any of these phases in equilibria in the ternary system is very close to its composition in the binary system. The set of data in Table 2 was thus plotted into the calculated phase diagram shown in Fig. 4, together with data collected from literature [5-9].

Table 2 – Magnesium content (wt %) of the phases at the limits of the microstructural domains in Fig. 3.

(Al)	β		ε		γ		(Mg)
5.8	36.0	36.4	41.5	40.6	50.5	58.0	94.1

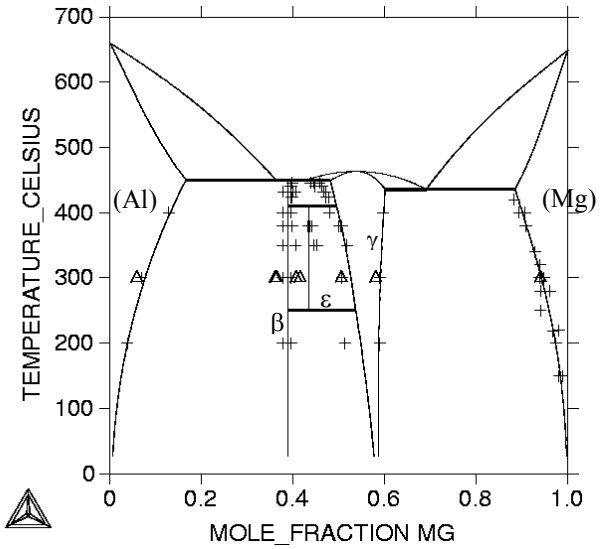

Figure 4 – Al-Mg phase diagram with experimental phase compositions from literature (crosses) and from Table 2 (triangles).

DTA results

Fig. 5 presents the DTA records obtained on cooling alloys A30, A45 and A70 at a scanning rate of 2.5 $K.min^{-1}$. There is a first thermal arrest, which appears at about 700 °C for all three alloys. An intermediate arrest shows up for alloys A30 and A70 but not for alloy A45. The final arrest is marked in any case, with even some recalescence for alloy A30. The records obtained from other scanning rates were similar for each alloy. Moreover, examination of the microstructure of each of the DTA samples confirmed similar microstructural features to the as-cast samples, although large primary Mg_2Si crystals were found in the upper part of some samples. It is thus clear that the high temperature arrest is associated with the formation of Mg_2Si and the intermediate arrest with the growth of (Al) for alloy A30 and the growth of (Mg) for alloy A70. The final arrest corresponds to the formation of β for alloy A30 and the formation of γ for both of alloys A45 and A70.

Based on the DTA records, an attempt was made to characterise the temperature of the final invariant reaction undergone by each alloy. Fig. 6 compares the DTA records obtained at various scanning rates in a temperature range across all possible solidification events for alloy A30. Upon heating, the very start of melting should correspond to the temperature at which the signal deviates

from the nearly horizontal basal line. This temperature appears not to be sensitive to the heating rate and was found equal to 448±1°C for alloy A30, 458±1°C for alloy A45 and 436±1°C for alloy A75. The peak temperature is another characteristic temperature and was found to shift to a higher value as the heating rate was increased. Upon cooling, the temperature corresponding to the start of the final reaction recorded by the DTA is influenced by the undercooling experienced by the material. So, the peak temperature, which in this case was found to shift to a lower value as the scanning rate was increased, is more useful as a characteristic temperature. A particular feature is observed in the case of alloy A30 where the peak is seen to split into two parts, a main peak and a marginal one. This feature will be further discussed below.

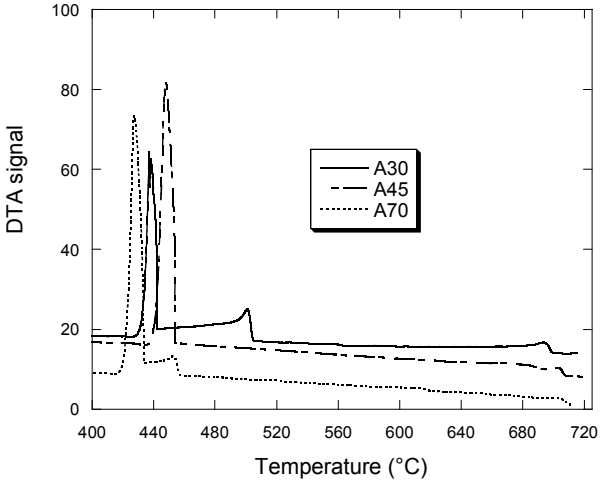

Figure 5 - DTA records obtained on cooling alloys A30, A45 and A70 at 2.5 K.min^{-1}.

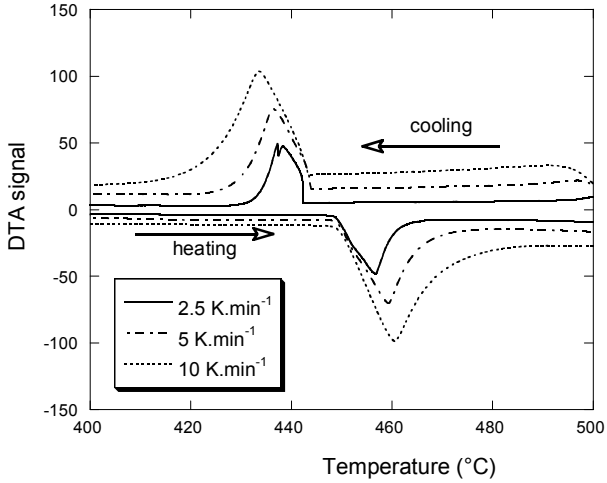

Figure 6 - DTA records for alloy A30 at various scanning rates in the temperature range of the final invariant reaction.

The characteristic temperatures, thus evaluated, are plotted in Fig. 7. Two series of DTA were made for alloy A30 and these are represented with empty triangles either upwards or downwards. The temperature of the second peak on cooling, when present, has been added with solid triangles. It was found that a linear relationship could be drawn through the peak temperature data against the square root of the scanning rate for each series. Furthermore, the resultant linear relationships extrapolate well to the experimental temperatures for the very start of melting of each alloy studied which have been plotted on Fig. 7 at a zero scanning rate. It is satisfying to notice that the absolute values of the slope of these lines are all very similar, indicating that the experiments are reproducible although a new sample was used in each run.

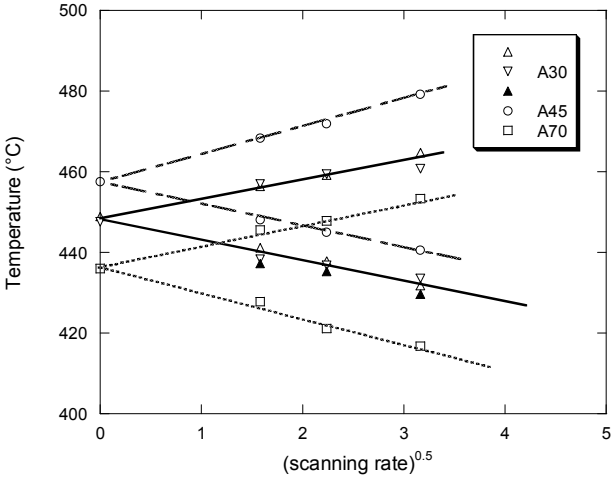

Figure 7 - Effect of scanning rates on the characteristic temperatures of the peak related to the final invariant reaction.

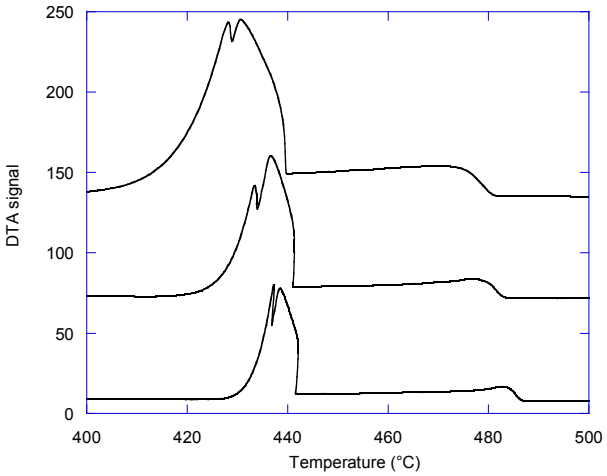

Figure 8 - DTA records for alloy D30 at cooling rates of 2.5, 5 and 10 $K.min^{-1}$.

At first glance, it was thought that the marginal peak recorded on the DTA curve of alloy A30 could be an artefact due to inhomogeneous temperature in the sample. This assumption was ruled out as it was never observed with alloys A45 and A70. The transformation is supposed to be the three phase invariant reaction, where some undercooling is required for the nucleation of new Mg_2Si crystals as the primary crystals of Mg_2Si have all become enveloped within (Al) or β. Accordingly, as can be inferred from Fig. 7, the potential linear relationship between the marginal peak temperature and scanning rate, represented by solid triangles in Fig. 7, would extrapolate to a lower temperature than the estimated incipient melting temperature. These hypotheses are supported by the fact that the marginal peak is well observed for alloy D30 for all three cooling rates, as illustrated in Fig. 8. The DTA samples of alloy D30 showed much more small precipitates than did the as-cast samples. As can be seen from Fig. 9(a), they are present in some regular patterns. Apparently, they were formed during the eutectic reaction. However, solid-state diffusion may have affected the solidification structure as very few (Al) phases have been found in the eutectic areas. As shown in Fig. 9(b), clear signs of growth of β at the expenses of the (Al) phase are observed in samples after a DTA run.

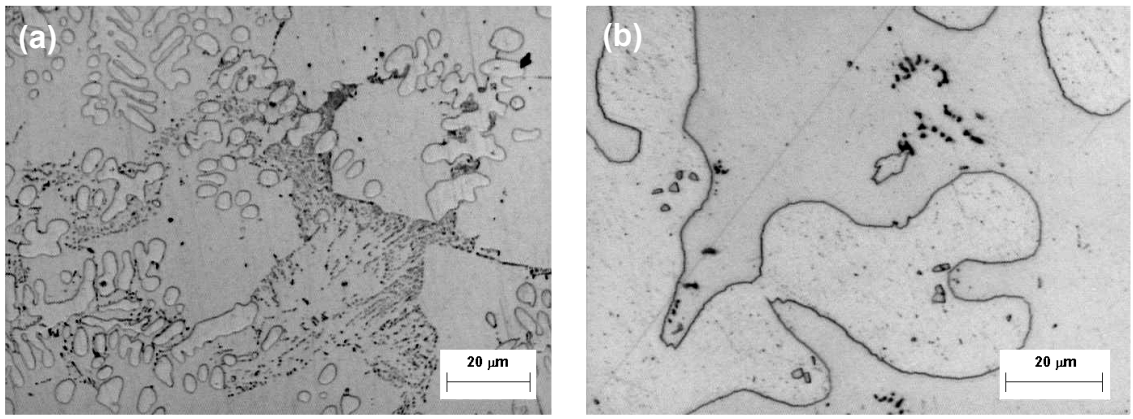

Figure 9 – Optical micrographs showing the microstructure of alloy D30 after a DTA run.

Summary

Solidification paths of Mg-rich Al-Mg-Si alloys finish on ternary eutectics located very close to the Al-Mg side of the composition triangle. These eutectics involve Mg_2Si and two phases of the Al-Mg system. The silicon content in any of these Mg-Al phases in the ternary eutectics has been found lower than 0.1 wt%. The temperatures of two of these ternary eutectic reactions, i.e. liquid ↔(Al)+β+ Mg_2Si and liquid↔(Mg)+γ+ Mg_2Si, have been determined to be at about 448 °C and 436 °C respectively by DTA.

Acknowledgements

Part of this study is supported by ESA through the MICAST programme under contract 14347/00/NL/SH. Thanks are due to M. Palm (MPI-E Düsseldorf) for WDS measurements and to L. Ratke and S. Steinbach (Institute for Space Simulation, DLR, Germany) for providing alloys.

References

[1] Lacaze J. and Valdes R., communication at the TOFA meeting, Vienna, 2004

[2] "Thermochemical database for light metal alloys", ed. I. Ansara, European Commission, 1995

[3] http://pro.wanadoo.fr/carine.crystallography/

[4] Villars P., "Pearson's Handbook Desk Edition", ASM international, 1997

[5] E. Schurmann,Giesserei-Forschung, 32, 163-174, 1980

[6] P. Liang et al., Z. Metallkd, 89, 536-540, 1998

[7] M.I. Zacharowa, W.K. Tschikin, Zeitschrift fur Physik, 95, 769-777, 1935

[8] E.Schimd, G. Siebel, Zeitschrift fur Physik, 85, 36-55, 1933

[9] P. Saldau, M. Zamotorin, Journal of the Institute of Metals, 48, 221-226, 1933